**ZULFAQAR Journal of Defence Science, Engineering & Technology**
e-ISSN: 2773-5281
Vol. 6, Issue 1(2023)
DOI: https://doi.org/10.58247/jdset-2023-0601-03
Journal homepage: https://zulfaqarjdset.upnm.edu.my

# ISOTROPIC AND ANISOTROPIC POLARIZATIONS OF MAGNETORHEOLOGICAL ELASTOMER

**Normidatul Salwa Sobri[a], Danesh Rajandran[a], Khisbullah Huda[a]*, Nur Akmal Hanifah[a], Zulkifli Abd Kadir[a], Mohd Sabirin Rahmat[b]**

[a] Department of Mechanical Engineering, Faculty of Engineering, National Defence University of Malaysia, Sg. Besi Camp, 57000 Kuala Lumpur, Malaysia
[b] Faculty of Engineering and Built Environment MAHSA University, Jenjarom, Selangor

**ARTICLE INFO**

**ARTICLE HISTORY**
Received: 30-10-2023
Revised: 15-01-2023
Accepted: 20-02-2023
Published: 30-06-2023

**KEYWORDS**
MRE
Isotropic
Anisotropic
Force absorption

**ABSTRACT**

The purpose of this research is to investigate the effect of varying currents injected into the coil during the curing process of magnetorheological elastomer (MRE) fabrication. In preparing MRE material, two types of MRE can be developed based on the curing process method fabrication which is isotropic and anisotropic. In this study, an anisotropic MRE is fabricated. The process of anisotropic MRE material is performed by applying the input current to the MRE material during the curing process. Firstly, the simulation is conducted by using the finite element magnetic method (FEMM) to investigate the magnetic field intensity. The magnetic field intensity is evaluated by varying the MRE parameters such as the number of coils turns, coil bobbin, the diameter of coil and input current applied to the coil. Then, the parameters are used for the MRE material fabrication process in preparing the optimum performance of anisotropic MRE. In this study, the three MRE designs are developed. The two designs of MRE are developed for anisotropic types and another one for isotropic type. The isotropic types are developed for comparing their capability performance to absorb the impact energy. To test the performance between anisotropic and isotropic, an impact test rig is used. The performance of anisotropic MRE is evaluated by comparing each input current applied to the MRE coil in the form of force-time characteristics.

## 1.0 INTRODUCTION

Magnetorheological elastomer (MRE) is categorized as smart materials whose rheological properties can be altered reversibly and rapidly by the presence of external magnetic force. MRE is a rubber-like material and applying a magnetic field can alter its properties. Asadi [1] stated that MREs usually contain magnetic particles which are micron-sized and distributed in a non-magnetic matrix. Damping coefficient is always related to MRE and needs to be taken under consideration when designing them. The MRE are widely used as dampers and absorbers in mechanical engineering, architecture, and military industrial domains because they have mechanical properties critical to engineering use. MREs are frequently employed as dampers and absorbers in mechanical engineering, architecture, and defence technology fields because they have mechanical properties essential to engineering application [2-6]. MREs are mostly employed in the defence field for gun recoil force and suspension systems in military ground vehicles.

MREs consist of pure iron, carbonyl iron or cobalt powder as the magnetic particles. The carrier fluid is usually either silicon or mineral oil. There are several different systems for MR materials, such as MR fluid, MR elastomer, MR foams and MR gels. Generally, MRFs are soft-magnetic particles that have high magnetic permeability and small hysteresis. These characteristics cause MRFs to have better shear viscosity and yield stress which is dependent on strength of the magnetic field and adhesion of micron-

*Corresponding Author | Huda, K. | k.huda@upnm.edu.my

sized magnetic particles. The advantages of using them are less noisy operation, their responsiveness on insensitivity to small amounts of impurity or dust, and easy to be handled and controlled [7-8].

Solid-state MREs overcome the disadvantages of MRFs. Viscoelastic properties of MRE can be altered under an applied magnetic field. This characteristic is alike to the MRF, but MRE is more of a solid form [9-10]. In addition, MREs generally consist of rubber matrix, additives, and magnetic carbonyl iron (CI) particles when the magnetic field is applied. This enhances the hardness, elastic modulus, and shear modulus. In past decades, MREs are utilized in three main categories which are vibration reduction, noise reduction and sensor devices. Hence, MREs have been a great positive impact on various engineering applications [11]. MREs can be divided into two which are isotropic and anisotropic MRE depending on magnetically polarized particle arrangement in them. For isotropic MRE, polarized particles are distributed uniformly so that the physical characteristics of the MRE is homogenous in every direction. Anisotropic MRE has their polarized particles arranged along the magnetic field direction when being manufactured [12-14].

Many studies on MREs have been done throughout the past years. Most of the researchers have focused on the general study, composition, and fabrication of MREs [15]. Input current effects during the curing process of anisotropic MRE have been studied on a very small scale and that too is not as a main objective of study. Input currents in anisotropic MRE should be tested if it is equally important as other aspects that have already been investigated [16]. This testing might prove to be imminent in affecting the properties of an anisotropic MRE. Therefore, this study will test the implications of varied current on rheological properties of anisotropic MRE with the presence of isotropic MRE as a standard.

## 2.0 METHODOLOGY

The relationship between varied current and MRE properties are considered in this study. Firstly, the simulation on MRE in simulating the magnetic field intensity is performed using finite element method magnetics (FEMM) [7]. Several inputs that need to be set such as materials selection and design parameters. Selecting materials and identifying their composition is imminent because it is going to be kept constant for the whole experimental process in this study. After obtaining the optimum design, the next process is preparing the MRE and testing using a drop impact test. The overall methodology of this study is shown in Figure 1.

The study begins by determining the research requirements, as shown in Figure 1. The study's underlying research includes the composition of MRE, the link between MRE and changing currents, and the effects of EMF on MRE. The next step is to define the goals of the study and conduct a literature review on the impacts of using current during the curing process in the manufacture of MRE. Following that, anisotropic and isotropic MRE were fabricated, and a drop impact test with variable current was conducted. The data will be discussed based on the experimental outcomes. Finally, the entire conclusion of the study is achieved.

*Corresponding Author | Huda, K. | k.huda@upnm.edu.my 

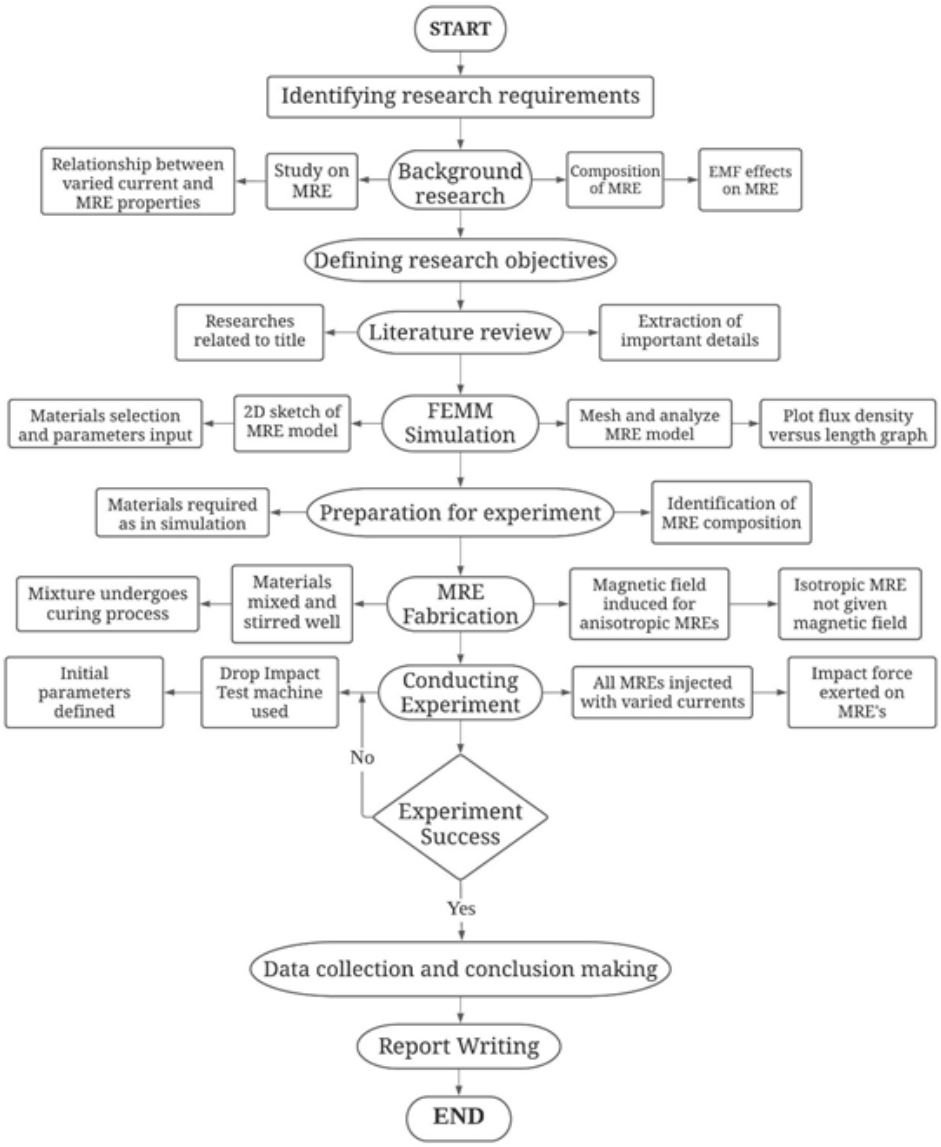


Figure 1. Methodology of the study

## 2.0 SIMULATION IN FEMM

The finite element method magnetics (FEMM) software was used to simulate the previously drafted magnetorheological elastomers. It is imminent in analysing the magnetic flux distribution of the MREs drafted besides being able to choose the most suitable one according to requirements. An MRE model is simulated with three amounts of varied current supply to ease the range selection process. In the FEMM software, the grids spacing is set to 10 along with the SI unit in millimetres. A 2-dimensional cross-section of the MRE is sketched. After sketching, material selections are determined and exported from the available material library under the properties tab. 1020 steel which is low carbon steel under soft magnetic materials is chosen for the design due to its low cost and vast availability [17]. The 0.8 mm copper magnet metric wire with 3000 turns is used as the coil selection where the varied current in series is injected into it. An air boundary is created around the MRE design with standard properties and a linear B-H relationship. Figure 2 shows the 2-D sketch of the MRE design through FEMM software.

The simulated MRE model has then meshed with 7671 nodes as illustrated in Figure 3. The figure also shows the after effect of meshing done on the MRE design. The analysis of the meshed design will be further investigated in the results section. The result from the analysis will allow a range of amount of current exhibiting the maximum flux density of MRE to be chosen and used in this study. Preparation of materials and apparatus will be done as a pre-fabrication step.

*Corresponding Author | Huda, K. | k.huda@upnm.edu.my 

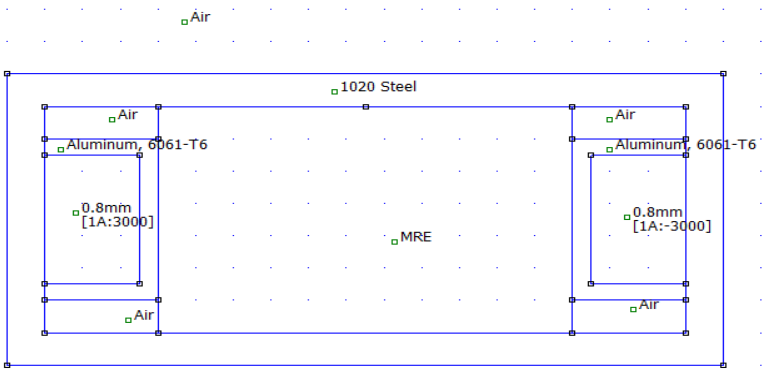


Figure 2. 2-D model of MRE sketch in FEMM software

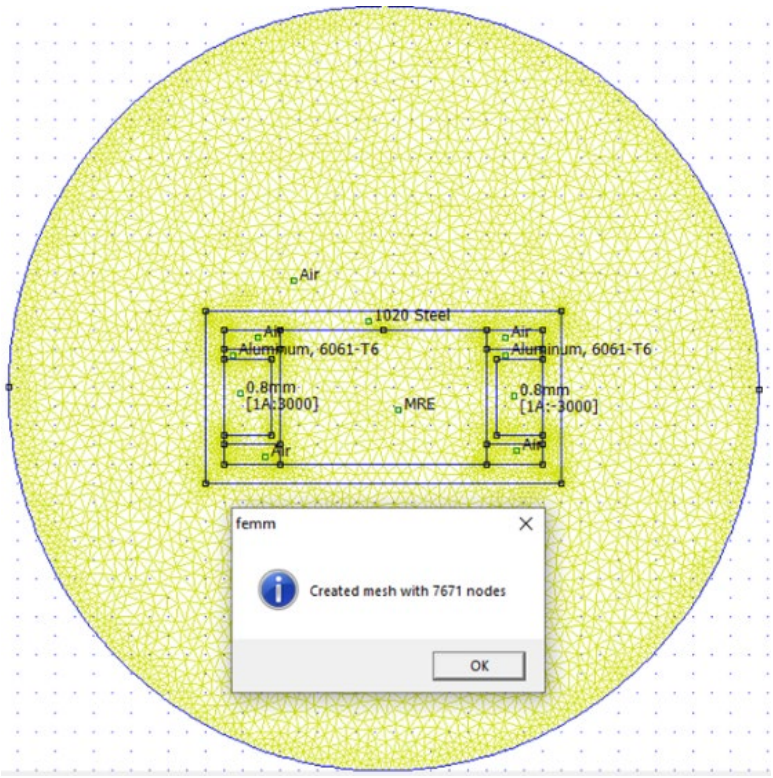


Figure 3. Mesh of MRE model with 7671 nodes

1.0

The relationship between electricity and magnetism is known as electromagnetism. A changing magnetic field creates an electrostatic force. A magnetostatic field is created when an electric field changes. The magnetic field is created by the motion of electric charges, such as current, which produces a magnetic force in magnets. The magnetic flux density use in this study is obtained from the simulation, and the magnetic flux density $\beta$ at the centre of the coil (maximum value) can be calculated as:

$$\beta = \frac{\mu N I}{\sqrt{4r^2 + l^2}} \tag{1}$$

where $\beta$ is the magnetic flux density or magnetic inductance (tesla, T or Weber/m2, Wb/m2), $\mu$ is the permeability of the material in the field (N/m2 ), $N$ is the number of turns on the excitation coil (turn, t or can be considered as unitless), $I$ is the current enclosed in the coil in each turn (A), $r$ is the radius of the wire (m), and $l$ is the length of the solenoid (m).

## 2.1 Fabrication Process of MRE

After simulation works have been completed, the next process is the fabrication of MRE as shown in Figure 8. The composition of all the MRE is set to be 70% ferrous particle and 30% silicon rubber. Two

*Corresponding Author | Huda, K. | k.huda@upnm.edu.my 

types of particle sizes are chosen namely 20-μm and 40 μm. Firstly, all the required equipment and materials are prepared for fabrication. Then, the electronic balance is on and set to tare. The container for materials mixing is placed on the electronic balance and the weight is set to tare again. Next, 21 grams of the ferrous particle of either 20-μm or 40-μm are filled in the container. After that, the electronic balance is set to tare before adding 9 grams of room temperature vulcanization (RTV) silicone rubber into the container. After adding, both the ferrous particle and RTV silicone rubber are mixed thoroughly for an even mixture without any leftovers of ferrous particle. After stirring, the electronic balance is set to tare and 0.27 grams of adhesive is added to the mixture.

The MRE mould is sprayed with sufficient silicone spray mould because it acts as a releasing agent later when the MRE is taken out from its mould. After that, the mixture is poured into the MRE mould. Then, magnets are placed and sealed in the moulds, and the MRE is given magnetic fields by placing two magnet moulds on the top and bottom of the MRE. These magnets give a magnetic field to the MRE and make it anisotropic. Finally, the MRE together with the magnets are isolated and left to dry for at least 24 hours with a big dry battery being placed on it. For the isotropic MRE, no magnets are placed on them. The dry battery is placed on the MRE to minimize forming of air bubbles in the MRE. After the MRE is dried, it is taken out from the mould and kept aside in preparation for experimental testing. This same step of fabrication is carried out for all 20-μm and 40-μm ferrous particle MREs fabricated.

Figure 4. MRE specimen

### 2.2 MRE Experimental Testing

After the fabrication process, the experiment is conducted at the Universiti Pertahanan Nasional Malaysia (UPNM) Automotive Lab. The machine used to conduct this experiment is the Instron Drop Impact Machine along with the CEAST software as illustrated in Figure 9. The designed MRE device is to house all the fabricated MREs. The MRE specimen is then placed in a coil bobbin and connected to the power source and current supply. The experimental work is started with the impact weight in the machine being raised up until it reaches its release height. The impact weight is considered to be the force energy exerted onto the MRE specimen. The impact weight had a load cell attached to it to keep track of the time for the drop impact force test. The parameters of the impact test are tabulated in Table

The impact velocity for the tests is 2.0 m/s, according to Table 1. The minimum crashworthiness velocity was used to determine the impact velocity. When the value of impact velocity was entered into the CEAST software application, the impact energy and falling height were automatically calculated. The drop impact test on the MREs following the ASTM D2444 and ISO 3127.

*Corresponding Author | Huda, K. | k.huda@upnm.edu.my 

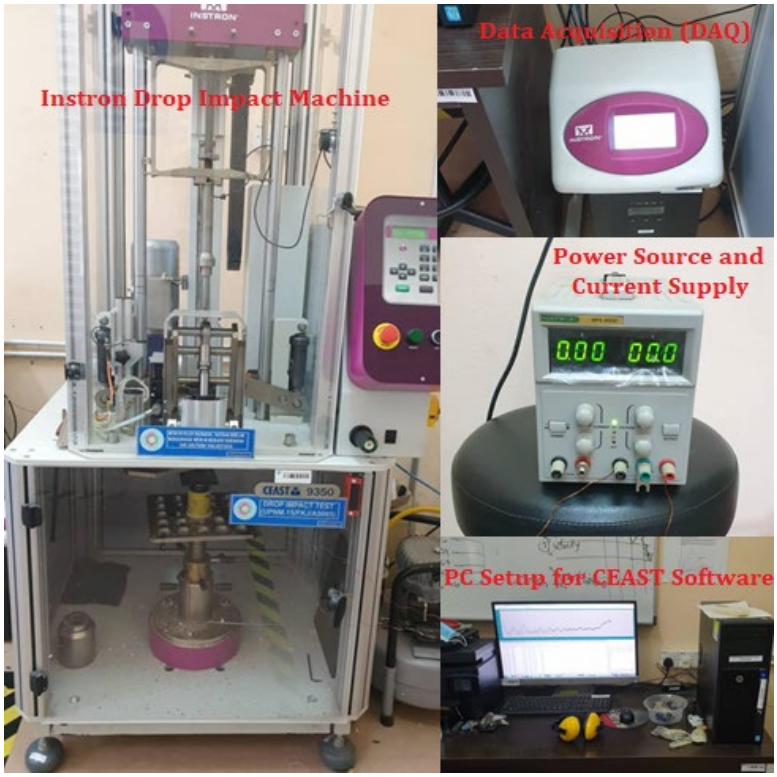


Figure 5. Experimental test setup

3 Table 1. Parameters for drop impact test

| Parameters | Value |
|---|---|
| Impact Energy | 11.00 J |
| Impact Velocity | 2.00 m/s |
| Falling Height | 204 mm |
| $T_{up}$ Holder Mass | 4.3 kg |
| $T_{up}$ Nominal Mass | 1.2 kg |
| Specimen Support | 3 mm |

## 3.0 RESULTS AND DISCUSSION

### 3.1 Simulation Results in FEMM

The MRE model after being meshed and analysed, the result can be viewed from the view results tab under the analysis section. From this analysis, the magnetic flux distribution under varied currents of the MRE can be viewed in detail. Besides the figure, a legend table is presented. The legend table consists of colours representing the intensity of magnetic flux around the MRE where it is arranged in descending order which is from the pink area to the light blue area. Figure 6 shows the magnetic flux distribution for the design of MRE.

Based on the result obtained, most of the magnetic flux intensity is absorbed by the 1020 steel surrounding both the coils in the model. This is because both the coils are surrounded by Aluminium 6061-T6 which is a soft non-magnetic material. Since it is non-magnetic, it will prevent uneven distribution of the magnetic field all around the coils. Hence, the maximum flux density will fall on the steel 1020 material beside the coils. Figure 7, Figure 8, and Figure 9 show the graphs of length versus magnetic flux density when the amount of current injected to the coils for 1A, 1.5A and 2A.

*Corresponding Author | Huda, K. | k.huda@upnm.edu.my 

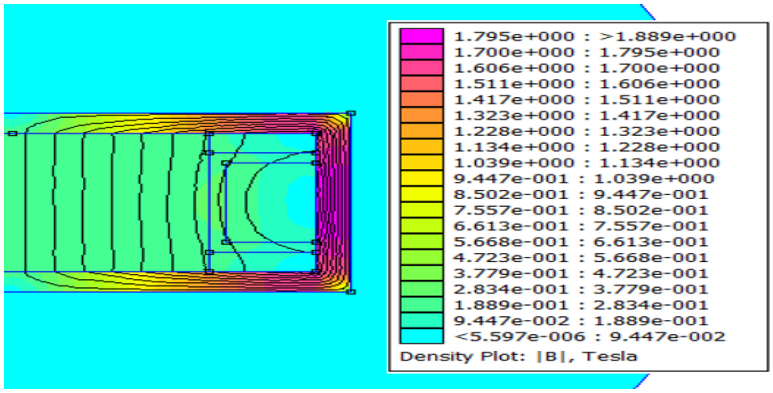


Figure 6. Analysis of MRE model in FEMM software

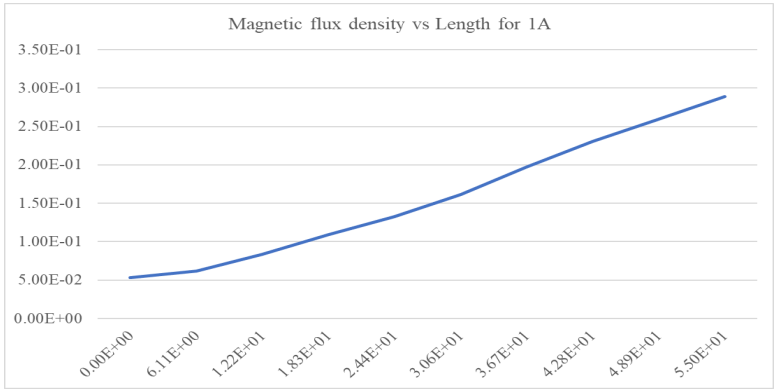


Figure 7. Graph of magnetic flux density versus length (mm) for 1 A current

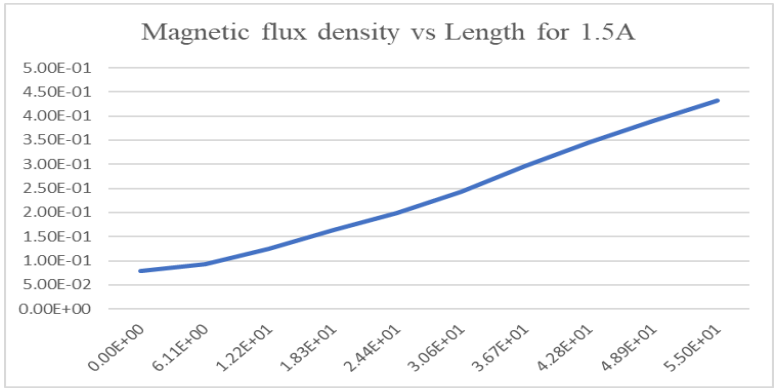


Figure 8. Graph of magnetic flux density versus length (mm) for 1.5 A current

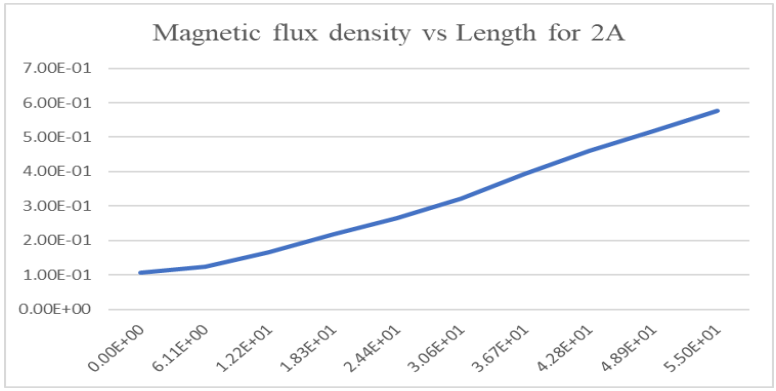


Figure 9. Graph of magnetic flux density versus length (mm) for 2 A current

Figure 7, Figure 8, and Figure 9 show the plot of magnetic flux density against length in inches when the current injected to the coils of MRE model were varied from 1A to 2A. The value of current that shows

*Corresponding Author | Huda, K. | k.huda@upnm.edu.my 

the maximum magnetic flux density will be set as the limit for experimental testing. Figure 7 shows the magnetic flux density when the coils are injected with 1A current. The maximum value obtained is approximately 0.3 Tesla. This is far from the theoretical maximum flux density which 53 is 1 Tesla. When the coils are injected with 2A current as shown in Figure 9, the maximum flux density obtained is close to 0.45 Tesla. This value also cannot be considered as it still does not approximate close to the 1 Tesla value needed.

### 3.2 Drop Impact Test Results

Figure 10 shows the experimental result for 40-µm isotropic MRE. Figures 11 and 12 are the graphs obtained from the experimental testing on 20-µm and 40-µm anisotropic MRE respectively. Once the experiment is completed, the data obtained for each input current value is collected in the Microsoft Excel software. After that, the data are imported into the Matlab R2021a software to plot the force vs time graphs. Matlab R2021a is used for plotting in order to get higher accuracy plots and readings required. The data used to plot the graph from the table is set from 0 milliseconds to 0.5 milliseconds, for each input current value of 40-µm isotropic MRE along with both 20- and 40-µm anisotropic MRE.

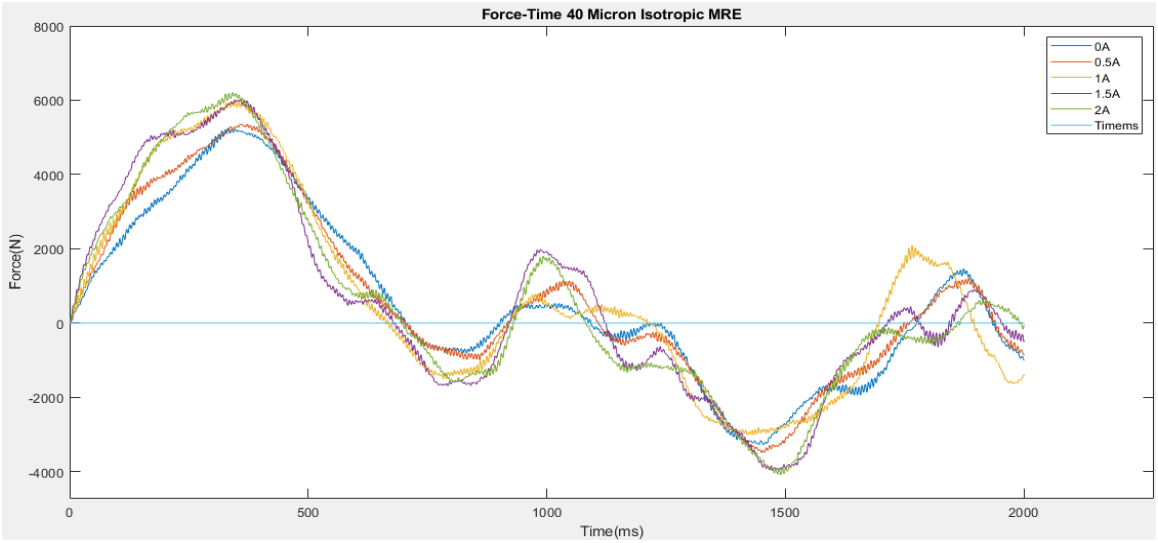


Figure 10. Graph of force vs time for 40-µm Isotropic MRE

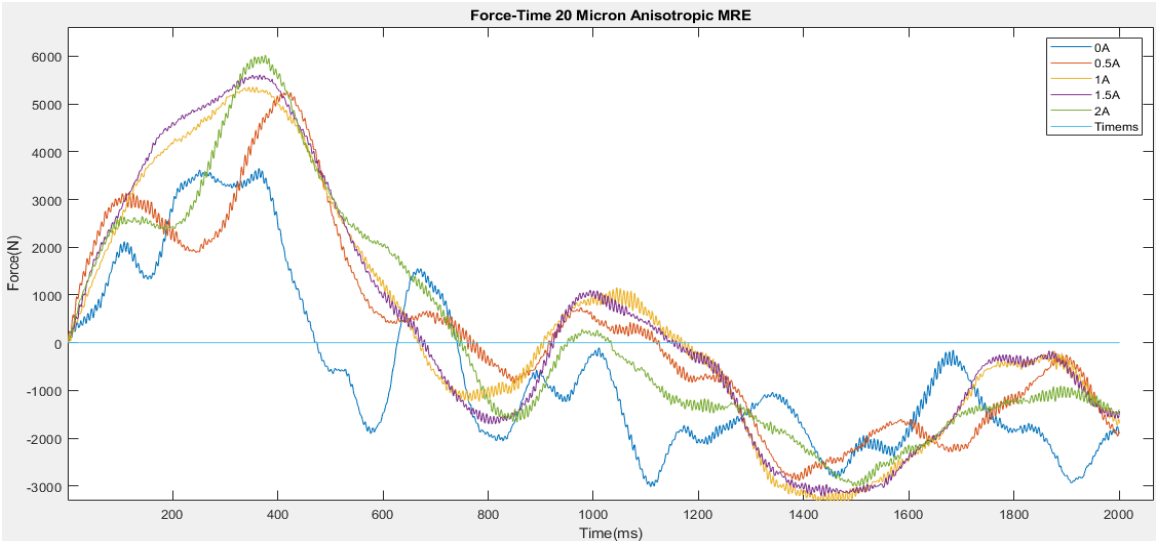


Figure 11. Graph of force vs time for 20-µm Isotropic MRE

*Corresponding Author | Huda, K. | k.huda@upnm.edu.my 

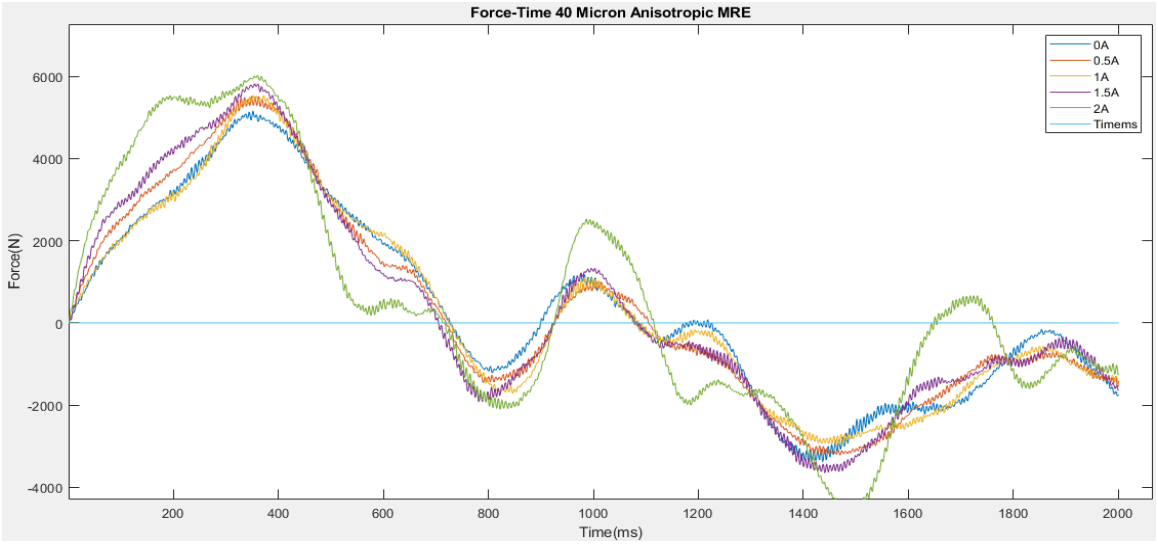


Figure 12. Graph of Force vs Time for 40 µm Anisotropic MRE

Tables 2, 3 and 4 show the maximum damping force obtained for each value of input current for 20-µm isotropic MRE, 20-µm anisotropic MRE and 40-µm anisotropic MRE, respectively. The damping force of each input current value was obtained by evaluating the highest amplitude obtained from the corresponding line in the graphs [18]. Generally, the trend of the damping force in all three tables are the same, they increase along with the increase of input current injected to the coils of MRE. Besides that, comparing the damping force for 20 µm anisotropic and 40-µm anisotropic MRE, the 40-µm anisotropic MRE presents a higher value of damping force from 0 to 1.5 amperes of input currents. Instead of that, the damping force acquired for input current value of 2A for these 2 MRE's are the same with 6021.73 N. Finally, the 40-µm isotropic MRE produced the highest value of damping force which is 6205.22 N.

Table 2. Input current and corresponding damping force for 40-µm isotropic MRE

| 40 µm Isotropic MRE | |
|---|---|
| Input Current, A | Damping Force, N |
| 0 | 5254.42 |
| 0.5 | 5354.51 |
| 1 | 5854.93 |
| 1.5 | 6038.42 |
| 2 | 6205.22 |

Table 3. Input current and corresponding damping force for 20-µm anisotropic MRE

| 20 µm Isotropic MRE | |
|---|---|
| Input Current, A | Damping Force, N |
| 0 | 3653.07 |
| 0.5 | 5254.42 |
| 1 | 5354.51 |
| 1.5 | 5604.72 |
| 2 | 6021.73 |

Table 4. Input current and corresponding damping force for 40-µm anisotropic MRE

| 40 µm Anisotropic MRE | |
|---|---|
| Input Current, A | Damping Force, N |
| 0 | 5154.34 |
| 0.5 | 5487.95 |
| 1 | 5537.99 |
| 1.5 | 5821.57 |
| 2 | 6021.73 |

*Corresponding Author | Huda, K. | k.huda@upnm.edu.my

Based on all the analyses that have been done on the MRE model, it is clear that the closest maximum magnetic flux density is given by the 2A current injected into coils and therefore it is the optimum current value. This maximum magnetic flux density exhibited by the optimum current of 2A will aid in the optimum working properties and characteristics of the MRE [19]. These findings are very important as they will prevent the coil from burning if injected with a very high amount of current during the experiment. Simulation of MRE in FEMM software has resulted in 2A current being determined to be the maximum input current value in this experiment. Therefore, the parameters used during simulation such as the 0.8mm diameter of the coil, 3000 number of coils turns, and the varied current range are considerable for the progress of this experiment towards success.

Isotropic MRE of 40-μm ferrous particles and anisotropic MRE of 20- μm and 40-μm ferrous particles were fabricated for experimental testing. The amount of input current injected into the coils of MRE during the experiment is varied in order of 0A, 0.5A, 1A, 1.5A and 2A. These values of currents were determined based on the findings from the FEMM simulation. 40-μm anisotropic MRE inhibited higher damping force values 5154.34 N, 5487.95 N, 5537.99 N and 5821.57 N for input currents of 0A, 0.5A, 1A and 1.5A respectively when compared to 20-μm anisotropic MRE which gave 3653.07 N, 5254.42 N, 5354.51 N and 5604.72 N of damping force values in the same order of input current values respectively. However, both 20 μm and 40-μm anisotropic MRE's resulted in 6021.73 N of damping force for input current of 2A. On the other hand, the 40-μm isotropic MRE inhibited higher damping force values of 5254.42 N, 5854.93 N, 6038.42 N and 6205.22 N for input current values of 0A, 1A, 1.5A and 2A respectively when compared with 40-μm anisotropic MRE but resulted in a lower damping force of 5354.51 N for input current of 0.5A.

Theoretically, anisotropic MREs impose a higher damping force than isotropic MREs [20-21]. This is because magnetic particles in anisotropic MRE are arranged in a chain-like structure as the magnetic field is induced with current whereas the magnetic particles in an isotropic MRE are uniformly dispersed [22-23]. MRE have a stronger impact absorption capability when they have a higher damping force response, which is also affected by different input current values [24-25]. In addition, significant impact absorption capability is necessary for MRE application in a military vehicle's cannon to reduce recoil force. As a result, finding the optimal ferrous particle size to improve the MRE's impact absorption performance is critical.

## 4.0 CONCLUSION

In this study, an MRE model was developed and simulated in the software. The MRE model was given three (3) amounts of varied current to obtain their maximum magnetic flux density. The optimum current that gives the nearest value to 1 Tesla was 2 Amperes. Simulation proved that when the amount of current injected increases, the magnetic flux density in the MRE increases. Next, 40-μm isotropic MRE, 20-μm and 40-μm anisotropic MRE were fabricated for the experimental testing. During the drop impact experiment, all the MREs were injected with varied current inputs of 0A, 0.5A, 1A, 1.5A and 2A. The maximum damping force of each input current value of all three MREs was presented in the experimental results. Tabulated data proved that the damping force of MREs increased with the increase of varied current injected into the coils of MRE during the experiment. Lastly, the anisotropic MRE has the highest damping force compared to isotropic MRE.

## 5.0 ACKNOWLEDGEMENT

The research has been carried out under Short Term Research Grant, UPNM/2021/GPJP/TK/3 provided by National Defence University of Malaysia (NDUM).

## List of Reference

[1] Khanouki, M. A., Sedaghati, R., & Hemmatian, M. (2019). Experimental characterization and microscale modeling of isotropic and anisotropic magnetorheological elastomers. Composites Part B: Engineering, 176, 107311.

[2] Zheng, J., He, X., Li, Y., Zhao, B., Ye, F., Gao, C., ... & E, S. (2020). Viscoelastic and magnetically aligned flaky Fe-based magnetorheological elastomer film for wide-bandwidth electromagnetic wave absorption. Industrial & Engineering Chemistry Research, 59(8), 3425-3437.

[3] Yunus, N. A., Mazlan, S. A., Choi, S. B., Imaduddin, F., Aziz, S. A. A., & Khairi, M. H. A. (2016).

*Corresponding Author | Huda, K. | k.huda@upnm.edu.my 

Rheological properties of isotropic magnetorheological elastomers featuring an epoxidized natural rubber. Smart Materials and Structures, 25(10), 107001.

[4] Wang, Y., Zhang, X., Chung, K., Liu, C., Choi, S. B., & Choi, H. J. (2016). Formation of core–shell structured complex microparticles during fabrication of magnetorheological elastomers and their magnetorheological behavior. Smart Materials and Structures, 25(11), 115028.

[5] Ahmed, M. M., Dhakal, H. N., Zhang, Z. Y., Barouni, A., & Zahari, R. (2021). Enhancement of impact toughness and damage behaviour of natural fibre reinforced composites and their hybrids through novel improvement techniques: A critical review. Composite Structures, 259, 113496.

[6] Minaev, A. J., Korovkin, J. V., Valiev, H. H., & Stepanov, G. V. (2020, November). Vibration and impact properties of magnetorheological elastomers. In IOP Conference Series: Materials Science and Engineering (Vol. 971, No. 4, p. 042059). IOP Publishing.

[7] Baltzis, K. B. (2010). The finite element method magnetics (FEMM) freeware package: May it serve as an educational tool in teaching electromagnetics?. Education and Information Technologies, 15, 19-36.

[8] Skalski, P., & Kalita, K. (2017). Role of magnetorheological fluids and elastomers in today's world. acta mechanica et automatica, 11(4), 267-274.

[9] Bocian, M., Kaleta, J., Lewandowski, D., & Przybylski, M. (2016). Impact absorption system based on MRE with Halbach array. Vibrations in Physical Systems, 27.

[10] Li, Y., Li, J., Li, W., & Du, H. (2014). A state-of-the-art review on magnetorheological elastomer devices. Smart materials and structures, 23(12), 123001.

[11] Kang, S. S., Choi, K., Nam, J. D., & Choi, H. J. (2020). Magnetorheological elastomers: Fabrication, characteristics, and applications. Materials, 13(20), 4597.

[12] Lee, C. W., Kim, I. H., & Jung, H. J. (2018). Fabrication and Characterization of Natural Rubber-Based Magnetorheological Elastomers at Large Strain for Base Isolators. Shock and Vibration, 2018(1), 7434536.

[13] Li, W. H., & Nakano, M. (2013). Fabrication and characterization of PDMS based magnetorheological elastomers. Smart materials and structures, 22(5), 055035.

[14] Li, W. H., Zhang, X. Z., & Du, H. (2013). Magnetorheological elastomers and their applications. In Advances in elastomers I: blends and interpenetrating networks (pp. 357-374). Berlin, Heidelberg: Springer Berlin Heidelberg.

[15] Hapipi, N., Mazlan, S. A., & Widodo, P. J. (2018, March). Design of magnetic Circuit Simulation for Curing Device of Anisotropic MRE. In IOP Conference Series: Materials Science and Engineering (Vol. 333, No. 1, p. 012008). IOP Publishing.

[16] Kaleta, J., Królewicz, M., & Lewandowski, D. (2011). Magnetomechanical properties of anisotropic and isotropic magnetorheological composites with thermoplastic elastomer matrices. Smart Materials and Structures, 20(8), 085006.

[17] Zhou, Y. (2016). Fatigue Properties Of Magnetorheological Elastomers And The Design Of Interfacial Layers To Improve Fatigue Life.

[18] Shuib, R. K., & Pickering, K. L. (2016). Investigation and modelling of damping mechanisms of magnetorheological elastomers. Journal of Applied Polymer Science, 133(13).

[19] Li, Y., Li, J., Tian, T., & Li, W. (2013). A highly adjustable magnetorheological elastomer base isolator for applications of real-time adaptive control. Smart Materials and Structures, 22(9), 095020.

[20] Soria-Hernández, C. G., Palacios-Pineda, L. M., Elías-Zúñiga, A., Perales-Martínez, I. A., & Martínez-Romero, O. (2019). Investigation of the effect of carbonyl iron micro-particles on the mechanical and rheological properties of isotropic and anisotropic MREs: Constitutive magneto-mechanical material model. Polymers, 11(10), 1705.

[21] Puente-Córdova, J. G., Reyes-Melo, M. E., Palacios-Pineda, L. M., Martínez-Perales, I. A., Martínez-Romero, O., & Elías-Zúñiga, A. (2018). Fabrication and characterization of isotropic and anisotropic magnetorheological elastomers, based on silicone rubber and carbonyl iron microparticles. Polymers, 10(12), 1343.

[22] Wahab, N. A. A., Mazlan, S. A., Hairuddin, K., & Zamzuri, H. (2015, November). Simulation study of electromagnetic circuit design in laminated magnetorheological elastomer isolator. In IOP Conference Series: Materials Science and Engineering (Vol. 100, No. 1, p. 012062). IOP Publishing.

[23] Wu, C., Cheng, C., Abd El-Aty, A., Li, T., Qin, Y., Yang, Q., ... & Guo, X. (2020). Influence of particles size and concentration of carbonyl iron powder on magnetorheological properties of silicone rubber-based magnetorheological elastomer. Materials Research Express, 7(8), 086101.

[24] Yang, J., Sun, S. S., Du, H., Li, W. H., Alici, G., & Deng, H. X. (2014). A novel magnetorheological elastomer isolator with negative changing stiffness for vibration reduction. Smart materials and structures, 23(10), 105023.

*Corresponding Author | Huda, K. | k.huda@upnm.edu.my 

[25] Ahamed, T. I., Sundarrajan, R., Prasaath, G. T., & Raviraj, V. (2014). Implementation of magneto-rheological dampers in bumpers of automobiles for reducing impacts during accidents. Procedia Engineering, 97, 1220-1226.

*Corresponding Author | Huda, K. | k.huda@upnm.edu.my 